Available online at www.sciencedirect.com
SCIENCE DIRECT®
Journal of Computational Physics 199 (2004) 339–354
JOURNAL OF COMPUTATIONAL PHYSICS
www.elsevier.com/locate/jcp

Dirichlet-to-Neumann boundary condition for time-dependent dispersive waves in three-dimensional guides

Dan Givoli [a,*], Igor Patlashenko [b]

[a] *Department of Aerospace Engineering and Asher Center for Space Research, Technion – Israel Institute of Technology, Haifa 32000, Israel*
[b] *Performance Group, EMC Corporation, 171 South Street, Hopkinton, MA 01748-9103, USA*

Received 22 July 2003; received in revised form 17 February 2004; accepted 17 February 2004
Available online 19 March 2004

Abstract

Exact Dirichlet-to-Neumann (DtN) boundary conditions on cross-sections of three-dimensional semi-infinite wave guides are derived. This enables the exact truncation of a wave guide to allow computations in a finite domain Ω. The DtN boundary condition is nonlocal in space but local in time. Practical implementation requires the truncation of the exact boundary condition by approximating an infinite sum with a finite sum, and by terminating an infinite recursion relation. The truncated condition is incorporated in a finite element scheme to solve the problem in Ω. The cross-section of the guide may have an arbitrary shape. The three-dimensional time-dependent *dispersive* wave equation is considered in the guide. The dispersion parameter is allowed to vary in the cross-section. All the results reduce immediately to the two-dimensional and to the one-dimensional cases. To the best of the authors' knowledge, this is the first time that an exact boundary condition is derived in the dispersive case, even in one dimension.

Keywords: Waves; Dispersion; Dirichlet-to-Neumann; Artificial boundary; Non-reflecting boundary condition; Finite elements; Auxiliary variables

1. Introduction

The Dirichlet-to-Neumann (DtN) map is a mathematical tool that can be used effectively to replace a problem given in a certain domain by an equivalent problem defined on the boundary (or part of the boundary) of that domain. See, e.g., [1] for a review on the subject and various applications. One important application is the numerical solution of problems in unbounded domains. In this case, the DtN map is used to truncate the infinite domain in an exact manner, so as to allow the computational solution of the problem in a finite domain. A more general family of schemes of this kind is the family of artificial boundary methods. An artificial boundary method consists in the following steps:

* Corresponding author. Tel.: +972-4-829-2308; fax: +972-4-829-3193.
E-mail addresses: givolid@aerodyne.technion.ac.il (D. Givoli), igorpt@sympatico.ca (I. Patlashenko).

0021-9991/$ - see front matter © 2004 Elsevier Inc. All rights reserved.
doi:10.1016/j.jcp.2004.02.011

(a) Introduce an artificial boundary $\mathscr{B}$, which divides the original unbounded domain into two domains: a finite computational domain Ω and an infinite residual domain D.
(b) By analyzing the problem in D, obtain a relation on $\mathscr{B}$ (exact or approximate) involving the unknown function u and its derivatives.
(c) Use this relation as a boundary condition on $\mathscr{B}$, to obtain a well-posed problem in Ω.
(d) Use a numerical method to solve the problem in Ω.

The relation obtained in step (b) and used as a boundary condition in step (c) is called an artificial boundary condition, or, in the context of wave problems, a non-reflecting boundary condition (NRBC). The latter name comes from the fact that such a boundary condition is aimed at eliminating the spurious reflection of waves from $\mathscr{B}$, which is otherwise present. See [2–4] for reviews on the subject.

The DtN boundary condition is an *exact* NRBC, and is based on the relevant DtN map. The latter is a linear operator, typically nonlocal, that is associated with the differential equation given in D and with the geometry of $\mathscr{B}$ and D (see [1]). Incorporating the DtN NRBC on $\mathscr{B}$ in a finite element (FE) formulation results in the DtN-FE method, which is a general numerical method for the solution of problems in unbounded domains. See [5] for details and references and [6] for recent advances.

A serious limitation of the DtN-FE method is that it is based on an analytic expression for the DtN map, which in turn may be difficult or impossible to derive for certain equations or configurations. The difficulty is similar to that of deriving the Green's function for a given problem. However, in those cases where the DtN map is available and is sufficiently simple (e.g., the Helmholtz equation with constant coefficients), the DtN-FE method has been shown to be very effective.

DtN-type NRBCs have been proposed mainly in the elliptic (or time harmonic) case. An exact NRBC for time-dependent waves was devised by Ting and Miksis [7,8] for three-dimensional (3D) waves exterior to a spherical artificial boundary. More recent exact NRBCs in the time-dependent case were proposed by Collino [9] for two-dimensional (2D) waves in rectangular domains, Guddati and Tassoulas [10] for time-dependent waves in a 2D wave guide, and Grote and Keller [11] and Hagstrom and Hariharan [12] for 3D waves exterior to a sphere. The Collino conditions and the Guddati–Tassoulas conditions are based on rational approximations, and are probably convergent (not only asymptotically correct) although this has not been proved in [9,10]. The Grote–Keller conditions and the Hagstrom–Hariharan conditions are convergent, but only in 3D.

Harari et al. [13] derived DtN boundary conditions for time-harmonic waves in 3D wave guides with an arbitrary cross-sectional shape. In this paper we generalized this work to the more difficult case of *time-dependent* waves. Moreover, we allow the medium to be *dispersive*. Wave dispersion makes the artificial boundary treatment yet harder. None of the exact NRBCs mentioned above is designed to deal with dispersion. In fact, to the best of our knowledge no exact NRBCs have been available for dispersive waves in *any* dimension. The new NRBC will be derived here for wave guides in 3D but is applicable to 2D and 1D as well. It is nonlocal in space (which is typical for DtN boundary conditions) but local in time. We allow the dispersion parameter to vary in the cross-section.

Very recently, Givoli et al. [14–16] proposed a high-order local NRBC for time-dependent dispersive waves. This NRBC is a practical implementation of the "theoretical" high-order Higdon NRBC [17]. In [15] it is shown that this NRBC is exact in a certain weak sense. The NRBC proposed in the present paper is entirely different, and is exact in the usual, stronger sense. On the other hand, it is relevant only for wave guide geometries, whereas the NRBC in [14–16] is much more general.

It should be remarked that practical implementation requires the truncation of the exact boundary condition by approximating an infinite sum with a finite sum, and by terminating an infinite recursion relation. Thus the actual boundary conditions used here are approximate. Moreover, the convergence of the scheme as the termination parameter approaches infinity is not proved here, although numerical experiments support it.

Following is the outline of the rest of this paper. In Section 2 we give the statement of the problem, and in Section 3 we derive the exact DtN boundary condition. In Section 4 we present the corresponding FE formulation. FE discretization leads to a system of ordinary differential equations in time, whose numerical solution we discuss in Section 5. In Section 6 we present a number of numerical examples with 3D and 2D wave guides. We conclude the paper with some remarks in Section 7.

2. Statement of the problem

We consider a 3D semi-infinite wave guide. The longitudinal coordinate of the wave guide is z, and x and y are coordinates in the cross-section. To make the computational domain Ω finite, we truncate the wave guide at a certain z location beyond all the "irregularities" of the problem (non-uniform cross section, inhomogeneities, nonzero initial conditions, nonlinearities, etc.). The truncation cross-section is denoted $\mathscr{B}$. For convenience we locate the coordinate origin there, so that $\mathscr{B}$ is the cross-section $z = 0$. The semi-infinite "tail" of the wave guide, which is assumed to be uniform in z, is denoted D, while its curved surface is denoted γ. A generic cross-section is denoted C. See Fig. 1.

Our goal is to find an exact boundary condition on $\mathscr{B}$ that will enable us to solve the problem in the finite domain Ω. To this end we consider the problem in D. We assume the following equation and boundary conditions:

$$C_0^2 \nabla^2 u = \ddot{u} + f^2 u \quad \text{in } D, \tag{1}$$

$$u = u_{\mathscr{B}} \quad \text{on } \mathscr{B}, \tag{2}$$

$$Su = 0 \quad \text{on } \gamma, \tag{3}$$

$$u \equiv 0, \quad \dot{u} \equiv 0 \quad \text{at } t = 0. \tag{4}$$

Eq. (1) is the dispersive (Klein–Gordon) equation, where C_0 is the reference wave speed and f is the dispersion parameter. A superposed dot indicates differentiation with respect to time t. In (2), $u_{\mathscr{B}}$ is a given though *arbitrary* function on $\mathscr{B}$, and S is a boundary operator which does not depend on z (such as the identity or the normal derivative). We assume C_0 to be constant in D, but we allow f to vary in the cross section, i.e., $f = f(x, y)$. These limiting assumptions apply only in the exterior domain D. In the finite computational domain Ω no such limitations exist in principle, since the problem is solved numerically there.

By solving the problem (1)–(4) we will be able to obtain a DtN-type boundary condition on $\mathscr{B}$. We recall [1] that in the simplest case the DtN boundary condition has the form

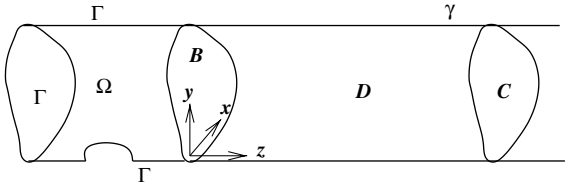

Fig. 1. A semi-infinite wave guide. The irregular region Ω is the computational domain, whereas D is a uniform "tail". A generic cross-section in the tail is denoted C, and the truncation cross-section separating Ω from D is denoted $\mathscr{B}$.

$$\frac{\partial u}{\partial z} = -Mu \quad \text{on } \mathscr{B}, \tag{5}$$

where M is an operator (the DtN map). In the time-dependent case, a DtN condition of the form (5) would usually be nonlocal in both space and time. Nonlocality in time means that the operator M involves an irreducible convolution integral, which in turn has distinct numerical disadvantages (see, e.g., [5]). However, locality in time may be achieved by extending (5) to the form

$$\boldsymbol{e}_1 \frac{\partial u}{\partial z} = -\boldsymbol{M}\boldsymbol{U} \quad \text{on } \mathscr{B}. \tag{6}$$

Here $\boldsymbol{U}$ is a vector whose entries are u and specially-defined auxiliary variables on $\mathscr{B}$, i.e.,

$$\boldsymbol{U}^{\mathrm{T}} = \{\, u \quad \phi_1 \quad \phi_2 \quad \cdots \quad \phi_{J-1} \,\}, \tag{7}$$

and $\boldsymbol{e}_1$ is the J-dimensional unit vector defined by

$$\boldsymbol{e}_1^{\mathrm{T}} = \{\, 1 \quad 0 \quad 0 \quad \cdots \quad 0 \,\}. \tag{8}$$

In (7) and (8), the $^{\mathrm{T}}$ denotes transposition. The DtN condition (6) becomes "exact" as J goes to infinity. We shall derive a DtN condition of the form (6) for the problem (1)–(4).

3. Derivation of the DtN boundary condition

We consider the problem (1)–(4) in D. We separate variables and write

$$u(x, y, z, t) = Y(x, y)U(z, t). \tag{9}$$

Then standard manipulation leads to

$$\frac{U''}{U} - \frac{1}{C_0^2}\frac{\ddot{U}}{U} = -\frac{\nabla^2 Y}{Y} + \frac{f^2}{C_0^2} \equiv \mu^2. \tag{10}$$

Here a prime denotes differentiation with respect to z, and μ is the separation constant. Eqs. (3) and (10) lead to the following eigenvalue problem in the cross-section C:

$$\nabla^2 Y + \left(\mu^2 - \frac{f^2}{C_0^2}\right) Y = 0 \quad \text{in } C, \tag{11}$$

$$SY = 0 \quad \text{on } \partial C. \tag{12}$$

This problem can be solved either analytically or (if not possible) numerically in the cross-section C, to yield the eigenvalues μ_n and the corresponding eigenfunctions Y_n, for $n = 0, 1, 2, \ldots$ Since the operator in (11) is self-adjoint, the eigenfunctions Y_n are orthogonal, namely

$$\int_C Y_n Y_m \, \mathrm{d}C = b_n \delta_{mn} \quad (\text{no sum}), \tag{13}$$

where δ_{mn} is the Kronecker delta, and b_n is the constant obtained from the integration when $m = n$. (Of course, the eigenfunctions can be normalized so that $b_n \equiv 1$.)

Now from (10) we get an equation for $U_n(z,t)$, i.e.,

$$U_n'' - \frac{1}{C_0^2}\ddot{U}_n - \mu_n^2 U_n = 0. \tag{14}$$

The solution u of the original problem is given by

$$u(x,y,z,t) = \sum_{n=0}^{\infty} Y_n(x,y)U_n(z,t). \tag{15}$$

The "Fourier coefficients" U_n in the expansion (15) in terms of the orthogonal functions Y_n are obtained from u via

$$U_n = \frac{1}{b_n}\int_C Y_n u \,\mathrm{d}C. \tag{16}$$

To obtain (16), multiply both sides of (15) by Y_m, integrate over C and use the orthogonality (13).

Now we introduce the family of *auxiliary functions* ϕ_{jn} (or $\phi_{j,n}$) using the following recursive definition:

$$\phi_{0n} \equiv U_n, \tag{17}$$

$$\phi_{j+1,n} \equiv \left(\frac{\partial}{\partial z} + \frac{1}{C_0}\frac{\partial}{\partial t}\right)\phi_{jn}, \tag{18}$$

for $j = 0,1,2,\ldots$ and $n = 0,1,2,\ldots$ This definition is reminiscent of that of ϕ_j used in [16], although there each auxiliary function had a single index j and the coefficient of $\partial/\partial t$ depended on it (i.e., $1/C_j$ rather than $1/C_0$).

From this definition and the fact that C_0 is constant it is easy to conclude that *each of the functions* ϕ_{jn} *satisfies a 1D wave equation like* (14), *namely,*

$$\phi_{jn}'' - \frac{1}{C_0^2}\ddot{\phi}_{jn} - \mu_n^2\phi_{jn} = 0. \tag{19}$$

This enables us to make the following calculation, analogous to the one used in [16]. First, (19) can be written as

$$\left(\frac{\partial}{\partial z} - \frac{1}{C_0}\frac{\partial}{\partial t}\right)\left(\frac{\partial}{\partial z} + \frac{1}{C_0}\frac{\partial}{\partial t}\right)\phi_{jn} - \mu_n^2\phi_{jn} = 0. \tag{20}$$

From (18) we then conclude

$$\left(\frac{\partial}{\partial z} - \frac{1}{C_0}\frac{\partial}{\partial t}\right)\phi_{jn} - \mu_n^2\phi_{j-1,n} = 0. \tag{21}$$

In deriving (21) we have replaced j by $j-1$ everywhere. Eq. (21) thus holds for $j = 1,2,\ldots$ and $n = 0,1,\ldots$ Now we add (18) and (21), note that the z-derivative term cancels out, and finally obtain

$$\frac{2}{C_0}\dot{\phi}_{jn} = \phi_{j+1,n} - \mu_n^2\phi_{j-1,n} \quad \text{on } \mathscr{B}, \tag{22}$$

for $j = 1,2,\ldots$ and $n = 0,1,\ldots$ Eq. (22) is a boundary condition on $\mathscr{B}$ for the auxiliary functions ϕ_{jn}. It is important to note that (22) *does not involve any z-derivatives*; hence the auxiliary functions ϕ_{jn} can be thought of now as if they are defined over $\mathscr{B}$ only, i.e., $\phi_{jn} = \phi_{jn}(x,y,t)$, despite the fact that we needed to consider their z-derivative in the derivation above.

The boundary condition (22) for $j = 1$ involves $\phi_{0n} \equiv U_n$. Since we do not desire U_n to appear explicitly in the formulation, we use (16) to express the U_n in terms of u on $\mathscr{B}$, i.e.,

$$\phi_{0n} \equiv U_n = \frac{1}{b_n} \int_{\mathscr{B}} Y_n u \, \mathrm{d}\mathscr{B}. \tag{23}$$

Substituting this in (22) for $j = 1$ yields

$$\frac{2}{C_0} \dot{\phi}_{1n} = \phi_{2n} - \frac{\mu_n^2}{b_n} \int_{\mathscr{B}} Y_n u \, \mathrm{d}\mathscr{B}. \tag{24}$$

It only remains to derive a boundary condition for u itself, which will be connected to the conditions given by (22) and (24). To this end we first note that from (18) with $j = 0$ and using (17) we have

$$\phi_{1n} = U_n' + \frac{1}{C_0} \dot{U}_n. \tag{25}$$

Now we calculate:

$$\begin{aligned} u'|_{\mathscr{B}} = u'(x,y,0,t) &= \sum_{n=0}^{\infty} Y_n(x,y) U_n'(0,t) = \sum_{n=0}^{\infty} Y_n(x,y) \left(\phi_{1n}(x,y,t) - \frac{1}{C_0} \dot{U}_n(0,t) \right) \\ &= -\frac{1}{C_0} \dot{u}(x,y,0,t) + \sum_{n=0}^{\infty} Y_n(x,y) \phi_{1n}(x,y,t). \end{aligned} \tag{26}$$

Here, the second equality follows from (15), the third equality follows from (25), and the last equality follows again from (9). Thus, we have

$$u' = -\frac{1}{C_0} \dot{u} + \sum_{n=0}^{\infty} Y_n \phi_{1n} \quad \text{on } \mathscr{B}. \tag{27}$$

The exact NRBC on $\mathscr{B}$ now consists of Eqs. (22), (24) and (27). To make it practical for computation we introduce two approximations:

1. We truncate the infinite sum over n in the equations above after N terms, for some given $N \geqslant 1$.
2. We terminate the recursive relations (18) by assuming

$$\phi_{J+1,n} \equiv 0 \tag{28}$$

for some given $J \geqslant 1$.

Thus we have $J(N+1)+1$ variables in our formulation: the function u and the auxiliary variables ϕ_{jn}, for $j = 1, \ldots, J$ and $n = 0, \ldots, N$. The following $J(N+1)+1$ equations, which are obtained from (22), (24), (27) and (28) constitute the corresponding NRBC on $\mathscr{B}$ for these variables:

$$u' = -\frac{1}{C_0} \dot{u} + \sum_{n=0}^{N} Y_n \phi_{1n}, \tag{29}$$

$$\frac{2}{C_0} \dot{\phi}_{1n} = \phi_{2n} - \frac{\mu_n^2}{b_n} \int_{\mathscr{B}} Y_n u \, \mathrm{d}\mathscr{B}, \quad n = 0, \ldots, N, \tag{30}$$

$$\frac{2}{C_0} \dot{\phi}_{jn} = \phi_{j+1,n} - \mu_n^2 \phi_{j-1,n}, \quad n = 0, \ldots, N, \;\; j = 2, \ldots, J, \tag{31}$$

$$\phi_{J+1,n} \equiv 0, \quad n = 0, \ldots, N. \tag{32}$$

This DtN-type NRBC is *nonlocal in space* due to the integral term in (30). However, it is *local* in time. Locality here means that no convolution integral in time appears in the formulation, so that the scheme does not require the *direct* use of "memory." This is in contrast to previous DtN formulations for unsteady waves, that involve convolution integrals and memory storage; see, e.g., [5]. The NRBC scheme based on the Kirchhoff integral [7,8] is also nonlocal in time, although the amount of required memory is fixed and does not grow in time. In the present scheme the locality in time, incorporated with the use of a standard two-step time integration scheme, implies that at each time step only information from the single previous time-step is used. Nevertheless, it should be realized that in a certain sense nonlocality in time of unsteady exact NRBCs is their fundamental property, that is only circumvented here computationally.

The question of convergence of the scheme using this NRBC as n and j increase naturally arises. Convergence of the infinite series in (29) as n approaches infinity is a consequence of the general theory of eigenfunctions. The convergence of the scheme as J goes to infinity is much more subtle. At present, we do not have a theory to support such a convergence. However, the numerical experiments presented in Section 6 as well as additional experiments not presented here demonstrate that the latter convergence indeed exists. In addition, the formulation presented here is reminiscent of (although not equivalent to) the high-order Higdon formulation presented in [15]. In the latter case, convergence is guaranteed under some general conditions, according to the theory developed by Higdon; see [17] and references therein, and see also discussion on this issue in [15].

We may try to analyze the behavior of the proposed NRBCs by transforming them and the whole problem into the frequency domain, namely by considering the time-harmonic case. Then the unsteady wave equation is replaced by the Helmholtz equation and the recursive relation (18) is replaced by

$$\phi_{j+1,n} \equiv \left(\frac{\partial}{\partial z} - ik \right) \phi_{jn}. \tag{33}$$

In the one-dimensional case the analysis is easy and leads to some constraints on the values of k and f in order to guarantee convergence for $J \to \infty$. (We thank the reviewer for bringing this to our attention.) However, the time-harmonic case, and hence the analysis mentioned above, does not fall into the framework of problems under discussion, since the important assumption of zero initial conditions in the exterior domain and on $\mathscr{B}$ is violated in this case. We remark that the same type of analysis can also be applied in the case of Higdon conditions [15,17]; in fact an operator similar to the one in (33) appears then. In that case, the constraints obtained by the one-dimensional time-harmonic analysis are clearly irrelevant in the time-dependent case. Thus, it seems that a simple time-harmonic analysis cannot provide useful information on convergence in the unsteady case using the NRBC (29)–(32).

The convergence analysis of the present scheme for increasing J values is left for theoretical investigation in future studies.

4. Finite element formulation

We consider the FE formulation of the problem in the computational domain Ω, using (29)–(32) as a NRBC on $\mathscr{B}$. The boundary of Ω on which physical boundary conditions are given (i.e., $\partial\Omega$–$\mathscr{B}$) is denoted Γ (see Fig. 1). In obtaining the FE formulation we shall assume that all the variables, namely u and all the ϕ_{jn}, are discretized using the same mesh and shape functions. Later in this section we shall comment on this assumption. We denote N_A and N_a the FE shape (basis) functions on the global and element level, respectively.

To fix ideas we consider the following problem in Ω:

$$C_0^2 \nabla^2 u = \ddot{u} + f^2 u - W \quad \text{in } \Omega, \tag{34}$$

$$C_0^2 \frac{\partial u}{\partial \nu} = H \quad \text{on } \Gamma, \tag{35}$$

$$\text{NRBC (29)–(32)} \quad \text{on } \mathscr{B}, \tag{36}$$

$$u = u_0, \quad \dot{u} = v_0 \quad \text{at } t = 0. \tag{37}$$

Here W and H are given functions (volume and boundary wave sources), u_0 and v_0 are given functions (initial conditions), and in (35) $\partial/\partial\nu$ is the normal derivative on Γ. It should be noted that all sources and initial conditions are assumed to be zero on the boundary $\mathscr{B}$ itself, namely the support of these functions is strictly *inside* Ω.

Eqs. (29), (34) and (35) lead, after standard FE discretization in space (see [18]), to the semi-discrete linear system

$$\boldsymbol{M}\ddot{\boldsymbol{d}} + \boldsymbol{C}\dot{\boldsymbol{d}} + \boldsymbol{K}\boldsymbol{d} = \boldsymbol{F} + \sum_{n=0}^{N} \boldsymbol{G}_n \boldsymbol{\phi}_{1n}. \tag{38}$$

Here $\boldsymbol{d}$ is the vector of nodal values of u, and $\boldsymbol{\phi}_{1n}$ is the vector of nodal values of ϕ_{1n}. The matrices $\boldsymbol{M}$, $\boldsymbol{K}$ and vector $\boldsymbol{F}$ are the standard FE arrays [18] and are not related to the NRBC on $\mathscr{B}$. On the element level their entries are given by

$$m_{ab}^e = \int_{\Omega^e} N_a N_b \, \mathrm{d}\Omega, \tag{39}$$

$$k_{ab}^e = C_0^2 \int_{\Omega^e} \nabla N_a \cdot \nabla N_b \, \mathrm{d}\Omega + f^2 \int_{\Omega^e} N_a N_b \, \mathrm{d}\Omega, \tag{40}$$

$$f_a^e = \int_{\Omega^e} N_a W \, \mathrm{d}\Omega + \int_{\Gamma^e} N_a H \, \mathrm{d}\Gamma. \tag{41}$$

Here the indices a and b denote element node numbers, the index e stands for an element number, and Ω^e is the domain of element e. The NRBC contributes only to the "damping matrix" $\boldsymbol{C}$ and to the "ϕ_{1n}-mass matrix" $\boldsymbol{G}_n$. On the element level, these arrays are calculated by

$$c_{ab}^e = C_0 \int_{B^e} N_a N_b \, \mathrm{d}\mathscr{B}, \tag{42}$$

$$(g_n^e)_{ab} = C_0^2 \int_{B^e} N_a Y_n N_b \, \mathrm{d}\mathscr{B}, \tag{43}$$

for nodes a and b on the boundary $\mathscr{B}$. (If either a or b is not on $\mathscr{B}$ the entry is zero.)

Eq. (30) in its original form would lead to a non-symmetric formulation. To avoid this, we multiply it throughout by Y_n to obtain

$$\frac{2}{C_0} Y_n \dot{\phi}_{1n} = Y_n \phi_{2n} - \frac{\mu_n^2}{b_n} Y_n \int_{\mathscr{B}} Y_n u \, \mathrm{d}\mathscr{B}. \tag{44}$$

Spatial FE discretization of (44) leads to the semi-discrete system

$$\boldsymbol{S}_n \dot{\boldsymbol{\phi}}_{1n} = \boldsymbol{R}_n \boldsymbol{\phi}_{2n} - \boldsymbol{P}_n \boldsymbol{d}. \tag{45}$$

The matrices $\boldsymbol{S}_n$ and $\boldsymbol{R}_n$ are calculated on the element level via

$$(s_n^e)_{ab} = \frac{2}{C_0} \int_{B^e} N_a Y_n N_b \, \mathrm{d}\mathscr{B}, \tag{46}$$

$$(r_n^e)_{ab} = \int_{B^e} N_a Y_n N_b \, \mathrm{d}\mathscr{B}. \tag{47}$$

Note that these matrices are in fact identical up to a scalar factor. The matrix $\boldsymbol{P}_n$ in (45) must be calculated on the global level due to the nonlocal nature of the integral term in (30):

$$(P_n)_{AB} = \frac{\mu_n^2}{b_n} \int_{\mathscr{B}} \int_{\mathscr{B}} N_A(\boldsymbol{x}) Y_n(\boldsymbol{x}) Y_n(\boldsymbol{x}') N_B(\boldsymbol{x}') \mathrm{d}\boldsymbol{x}' \, \mathrm{d}\boldsymbol{x}, \tag{48}$$

$$(P_n)_{AB} = \frac{\mu_n^2}{b_n} \left(\int_{\mathscr{B}} N_A Y_n \, \mathrm{d}\mathscr{B} \right) \left(\int_{\mathscr{B}} N_B Y_n \, \mathrm{d}\mathscr{B} \right). \tag{49}$$

Finally, FE discretization of Eq. (31) leads to the semi-discrete system

$$\boldsymbol{S}\dot{\boldsymbol{\phi}}_{jn} = \boldsymbol{R}\boldsymbol{\phi}_{j+1,n} - \boldsymbol{Q}_n \boldsymbol{\phi}_{j-1,n}, \quad j = 2, \ldots, J. \tag{50}$$

On the element level, the matrices $\boldsymbol{S}$, $\boldsymbol{R}$ and $\boldsymbol{Q}_n$ are calculated via

$$s_{ab}^e = \frac{2}{C_0} \int_{B^e} N_a N_b \, \mathrm{d}\mathscr{B}, \tag{51}$$

$$r_{ab}^e = \int_{B^e} N_a N_b \, \mathrm{d}\mathscr{B}, \tag{52}$$

$$(q_n^e)_{ab} = \mu_n^2 \int_{B^e} N_a N_b \, \mathrm{d}\mathscr{B}. \tag{53}$$

These three matrices are identical up to a scalar factor.

The FE formulation presented above allows, at least in theory, a general choice of the shape functions. Namely, different shape functions $N_a^{(j)}$ may be chosen for the different variables ϕ_j. However, it is advantageous to choose all the shape functions to be the same for all the variables, as done above. It should be noted that one has to be careful with the choice of the shape functions in a mixed FE formulation like the present one, since the Babuška–Brezzi (BB) condition of stability must be satisfied [18]. Fortunately, numerical experiments that we have performed show that equal-order interpolation, and in particular bilinear shape functions in Ω for u and linear one-dimensional shape functions on $\mathscr{B}$ for all the ϕ_j, is a stable combination. No locking or other convergence difficulties have been observed. The situation is somewhat similar to that of the mixed FE formulation devised in [19] for time-harmonic waves. Yet, the satisfaction of the BB condition is still to be proved mathematically.

5. Solution of the semi-discrete equations

The full system of semi-discrete equations is given by (38), (45), (50) and the FE nodal analogue of (32). We write these equations again for clarity:

$$\boldsymbol{M}\ddot{\boldsymbol{d}} + \boldsymbol{C}\dot{\boldsymbol{d}} + \boldsymbol{K}\boldsymbol{d} = \boldsymbol{F} + \sum_{n=0}^{N} \boldsymbol{G}_n \boldsymbol{\phi}_{1n}, \tag{54}$$

$$\boldsymbol{S}_n \dot{\boldsymbol{\phi}}_{1n} = \boldsymbol{R}_n \boldsymbol{\phi}_{2n} - \boldsymbol{P}_n \boldsymbol{d}, \quad n = 0, \ldots, N, \tag{55}$$

$$\boldsymbol{S}\dot{\boldsymbol{\phi}}_{jn} = \boldsymbol{R}\boldsymbol{\phi}_{j+1,n} - \boldsymbol{Q}_n \boldsymbol{\phi}_{j-1,n}, \quad n = 0, \ldots, N, \;\; j = 2, \ldots, J, \tag{56}$$

$$\boldsymbol{\phi}_{J+1,n} = \boldsymbol{0}. \tag{57}$$

A time-integration scheme is proposed now for the solution of this coupled system of ODEs. The subsystem (54) for $\boldsymbol{d}$ is of second order, and is discretized based on the Newmark family of schemes [18]. This family has two parameters, $0 \leqslant \beta \leqslant 1/2$ and $0 \leqslant \gamma \leqslant 1$, which control the accuracy and stability of the scheme. The subsystems (55) and (56) for $\boldsymbol{\phi}_{jn}$ have a first-order form and are solved using the generalized trapezoidal family of schemes [18], which involves one parameter $0 \leqslant \alpha \leqslant 1$.

The approximations of $\boldsymbol{d}$, $\dot{\boldsymbol{d}}$ and $\ddot{\boldsymbol{d}}$ at time-step m are denoted by $\boldsymbol{d}_m$, $\boldsymbol{v}_m$ and $\boldsymbol{a}_m$, respectively. Also, the approximations of $\boldsymbol{\phi}_{jn}$ and $\dot{\boldsymbol{\phi}}_{jn}$ at time-step m are denoted by $(\boldsymbol{\phi}_{jn})_m$ and $(\boldsymbol{V}_{jn})_m$, respectively. The time-step size is denoted Δt.

In predictor-corrector form, the proposed time-integration scheme (for advancing from time-step m to time-step $m+1$) is

Prediction:

$$\tilde{\boldsymbol{d}}_{m+1} = \boldsymbol{d}_m + \Delta t \boldsymbol{v}_m + \frac{\Delta t^2}{2}(1-2\beta)\boldsymbol{a}_m, \tag{58}$$

$$\tilde{\boldsymbol{v}}_{m+1} = \boldsymbol{v}_m + (1-\gamma)\Delta t \boldsymbol{a}_m, \tag{59}$$

$$(\tilde{\boldsymbol{\phi}}_{jn})_{m+1} = (\boldsymbol{\phi}_{jn})_m + (1-\alpha)\Delta t (\boldsymbol{V}_{jn})_m, \quad j = 1, \ldots, J, \;\; n = 0, \ldots, N. \tag{60}$$

Solution + correction for $\boldsymbol{d}$:

$$(\boldsymbol{M} + \gamma \Delta t \boldsymbol{C} + \beta \Delta t^2 \boldsymbol{K})\boldsymbol{a}_{m+1} = \boldsymbol{F}_{m+1} + \sum_{n=0}^{N} G_n (\tilde{\boldsymbol{\phi}}_{1n})_{m+1} - \boldsymbol{C}\tilde{\boldsymbol{v}}_{m+1} - \boldsymbol{K}\tilde{\boldsymbol{d}}_{m+1}, \tag{61}$$

$$\boldsymbol{d}_{m+1} = \tilde{\boldsymbol{d}}_{m+1} + \beta \Delta t^2 \boldsymbol{a}_{m+1}, \tag{62}$$

$$\boldsymbol{v}_{m+1} = \tilde{\boldsymbol{v}}_{m+1} + \gamma \Delta t \boldsymbol{a}_{m+1}. \tag{63}$$

Solution + correction for $\boldsymbol{\phi}_{1n}$:

$$\boldsymbol{S}_n (\boldsymbol{V}_{1n})_{m+1} = \boldsymbol{R}_n (\tilde{\boldsymbol{\phi}}_{2n})_{m+1} - \boldsymbol{P}_n \boldsymbol{d}_{m+1}, \quad n = 0, \ldots, N, \tag{64}$$

$$(\boldsymbol{\phi}_{1n})_{m+1} = (\tilde{\boldsymbol{\phi}}_{1n})_{m+1} + \alpha \Delta t (\boldsymbol{V}_{1n})_{m+1}, \quad n = 0, \ldots, N. \tag{65}$$

Solution + correction for $\boldsymbol{\phi}_{jn}, j \geqslant 2$:

$$\text{For } j = 2, \ldots, J, \tag{66}$$

$$\boldsymbol{S}(\boldsymbol{V}_{jn})_{m+1} = \boldsymbol{R}(\tilde{\boldsymbol{\phi}}_{j+1,n})_{m+1} - \boldsymbol{Q}_n(\boldsymbol{\phi}_{j-1,n})_{m+1}, \quad n = 0, \ldots, N, \tag{67}$$

$$(\boldsymbol{\phi}_{jn})_{m+1} = (\tilde{\boldsymbol{\phi}}_{jn})_{m+1} + \alpha\Delta t(\boldsymbol{V}_{jn})_{m+1}, \quad n = 0, \ldots, N. \tag{68}$$

Note the order in which these calculations are done in the scheme above at each time step. This order is designed so that in each calculation the maximal amount of information is available from previous calculations. Note, however, that in (61), (64) and (67), the predicted vector $(\tilde{\boldsymbol{\phi}}_{j+1,n})_{m+1}$ has been used rather than $(\boldsymbol{\phi}_{j+1,n})_{m+1}$, since the latter is not known at the current stage of the calculation. This may lead to a numerical instability or to poor accuracy. To avoid these, the whole solution process given by Eqs. (61)–(68) is repeated, within a time step, a number of times in an iterative manner. In each additional cycle use is made of the last computed $\boldsymbol{\phi}_{j+1,n}$ instead of $(\tilde{\boldsymbol{\phi}}_{j+1,n})_{m+1}$. Numerical experiments show that usually one additional cycle is needed to yield stable and accurate results.

It should be noted that the split time-integration scheme proposed above is not the only way to go about solving the system of semi-discrete equations. One other way is by a fully implicit scheme. In this case all the equations are solved simultaneously, taking into account all the coupling terms. This scheme is unconditionally stable, but at the same time involves a large non-symmetric system of equations, and is inconvenient from a programming point of view. The other extreme, namely that of a fully explicit scheme, may be possible too, although we have not considered such schemes in the present study.

6. Numerical examples

We now demonstrate the performance of the scheme described above with a number of examples. We consider a semi-infinite wave guide with a rectangular cross-section, as shown in Fig. 2. The cross-sectional dimensions are 3×3. We take $C_0 = 1$, and initially we assume that the medium is dispersion-free, i.e., $f = 0$. On the cylindrical boundary, defined by the four planar surfaces $x = 0$, $y = 0$, $x = 3$ and $y = 3$, we take a zero Neumann boundary condition (hard wall), i.e., $\partial u/\partial v = 0$. On the edge $z = 0$ we take the zero Dirichlet condition $u = 0$. There are no wave sources, so the whole problem is driven by the initial conditions. It should be noted in passing that as far as the treatment of the boundary $\mathscr{B}$ is concerned, there is no inherent difference between waves driven by sources or by initial conditions. Since we assumed that both sources and initial data are zero on $\mathscr{B}$, the information arrives to $\mathscr{B}$ only from within Ω. In the present example the initial velocity $\dot{u}$ is zero throughout Ω, but $u(x, y, z, 0) = u_0$ (see (37)) is nonzero in the region $0.9 \leqslant z \leqslant 1.5$ and varies in all three directions. In the z-direction u_0 changes piecewise-linearly (like a "hat"

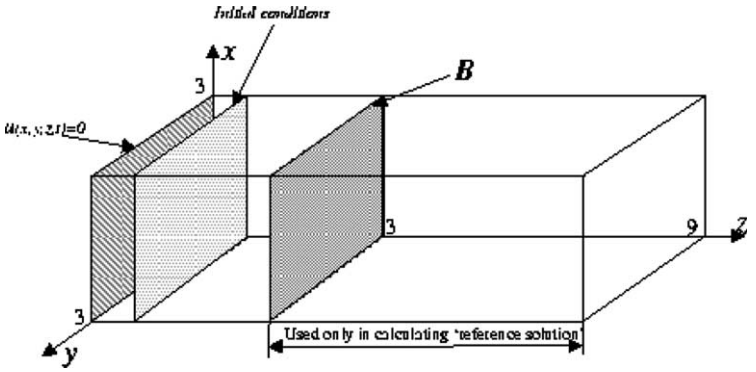

Fig. 2. The 3D rectangular wave guide problem.

function) from 0 at $z = 0.9$ to 1 at $z = 1.2$ to 0 again at $z = 1.5$. In the cross-section we consider three different variations of u_0:

$$\text{Case } 1 : u_0(x,y) = 1, \tag{69}$$

$$\text{Case } 2 : u_0(x,y) = \cos(\pi x/3)\cos(\pi y/3), \tag{70}$$

$$\text{Case } 3 : u_0(x,y) = (-(2/3)x^2 + (5/3)x)(-(2/3)y^2 + (5/3)y). \tag{71}$$

The first case is uniform, the second corresponds to a pure mode (eigenfunction), whereas the third is parabolic and thus consists of an infinite number of modes.

We truncate the wave guide by introducing the artificial boundary $\mathscr{B}$ at $z = 3$, as shown in Fig. 2. This defines the computational domain Ω which is a $3 \times 3 \times 3$ cube. As a reference solution to which we shall compare our results, we take the solution obtained by truncating the guide at $z = 9$. Thus, the reference computational domain is three times longer than Ω. During the simulation time waves will not reach $z = 9$ and thus the reference solution will be free from spurious reflection, and will be regarded as the 'exact solution'.

A mesh of 1000 bilinear finite elements ($10 \times 10 \times 10$) is used to discretize Ω. A mesh of 3000 bilinear elements of the same density is used for the reference solution. On the artificial boundary $\mathscr{B}$ we use the DtN boundary conditions described earlier with chosen parameters N and J (see below). In the time integration scheme we use the Newmark parameters $\beta = 0.25$ and $\gamma = 0.5$, the trapezoidal parameter $\alpha = 0.5$, and the time-step size $\Delta t = 0.01$.

Recall that J is the order of the NRBC which is also the number of auxiliary variables taken, whereas N is the number of eigenfunctions included in the DtN expansion. Since the cross-sectional eigenfunctions are two-dimensional, each $n = 0, \ldots, N$ represents a pair of modes in the x- and y-directions, i.e., $n = (n_x, n_y)$. We number the modes in the following fashion:

$$n = 0; 1; 2; \ldots \equiv (0,0); (1,0); (0,1); (1,1); (2,0); (0,2); (2,1); (1,2); (2,2); \ldots \tag{72}$$

Thus, for example, $N = 3$ includes the modes $\{(0,0); (0,1); (1,0); (1,1)\}$, namely all the modes with $n_x \leqslant 1$, $n_y \leqslant 1$, whereas $N = 8$ includes all the modes appearing in (72), namely the modes with $n_x \leqslant 2$, $n_y \leqslant 2$.

For Case 1 and Case 2 we took $J = 5$ and a varying N. As expected, in Case 1 the same numerical results were obtained for all values of N (since the exact solution in this case corresponds to the cross-sectional mode $N = 0$, and hence including additional modes in the DtN expansion does not change the accuracy), and in Case 2 the results did not depend on N for $N \geqslant 3$. In particular, we compared the errors generated by the $(N = 3, J = 5)$ DtN NRBC and by the Sommerfeld-like boundary condition which is the simplest NRBC possible (see, e.g., [2]). In Case 1, the relative maximal pointwise error on $\mathscr{B}$ was 0.48% for both NRBCs. In Case 2, the error was 8.33% for the Sommerfeld-like NRBC and 0.39% for the DtN condition.

Case 3 poses a more difficult problem since in this case the exact solution involves an infinite number of modes. Fig. 3 shows the solution u at time $t = 4$ and location $z = 3$ and $y = 3$, as a function of x. Since the wave speed is $C_0 = 1$, at time $t = 4$ the front of the wave already passed the artificial boundary. Four solutions are shown in the figure: the 'exact' solution, and the solutions corresponding to three combinations of N and J: $(N = 3, J = 1)$, $(N = 3, J = 4)$ and $(N = 8, J = 6)$. We see that the $(N = 8, J = 6)$ solution is indistinguishable from the 'exact' solution, whereas the other two numerical solutions contain a significant error. It is interesting to note that these two low-order solutions "bound" the exact solution along most of the x interval from different sides.

In Fig. 4 we compare the four solutions on $\mathscr{B}$ at time $t = 4$ by superposing the contour lines of the 'exact' solution on those of each of the numerical solutions. The improvement in accuracy achieved as N and J increase is apparent. The $(N = 3, J = 1)$ solution is completely off, the $(N = 3, J = 4)$ solution captures the qualitative behavior of the 'exact' solution correctly but with some spurious phase shifts, whereas the $(N = 8, J = 6)$ solution almost coincides with the 'exact' solution.

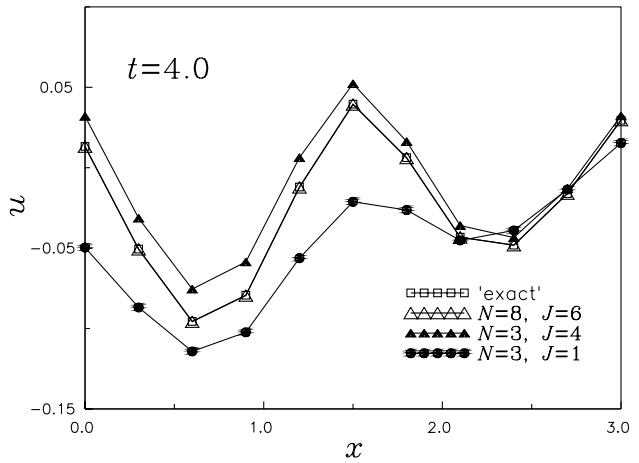

Fig. 3. The 3D wave guide problem: comparison of solutions along the x-direction at time $t = 4$ and location $z = 3$ and $y = 3$.

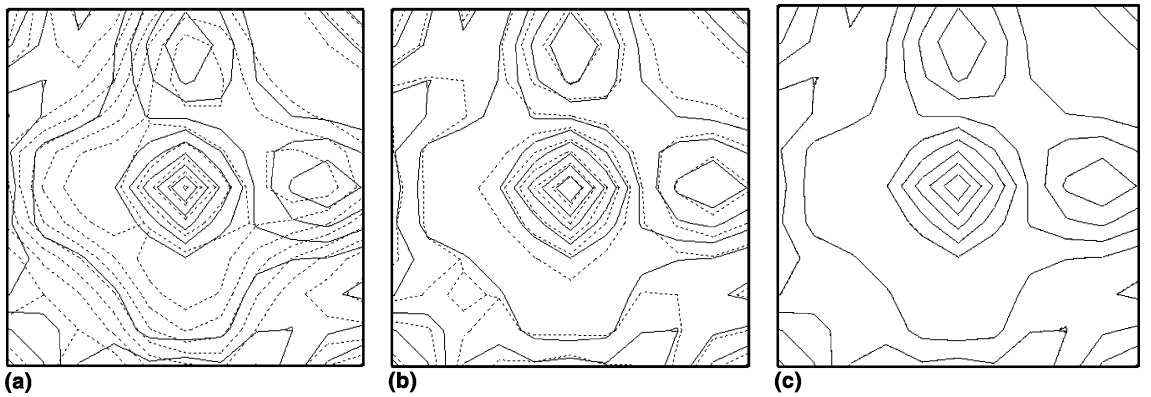

Fig. 4. The 3D wave guide problem: comparison, at time $t = 4$, of contour lines of the 'exact' solution on $\mathscr{B}$ with (a) the $(N = 3, J = 1)$ solution, (b) the $(N = 3, J = 4)$ solution, and (c) the $(N = 8, J = 6)$ solution. The 'exact' solution is represented by solid lines, whereas the solutions using the NRBCs are represented by dashed lines.

To further investigate the computational errors generated by the proposed scheme, we now turn into a simpler 2D problem. We consider a wave guide with a square cross-section, but this time the boundary and initial conditions, hence the solution itself, do not depend on x but only on y and z. The whole problem can be solved in a (y, z) semi-infinite strip of width $b = 3$. All the parameters remain the same as for the 3D problem considered previously, except that the initial condition for u is taken to be

$$u_0(y, z) = H(z) \cos(4\pi y/b), \tag{73}$$

where $H(z)$ is a "hat" function, varying piecewise-linearly from 0 at $z = 0$ to 1 at $z = 0.5$ to 0 again at $z = 1$, and is zero for $z \geqslant 1$. A 60×60 element mesh is used in the 3×3 computational domain Ω.

To measure the global error, we first define the error measure

$$\bar{E}^2(t) = \sum_{m=1}^{N_{\mathscr{B}}} (u(y_m, 0, t) - u_{\text{ex}}(y_m, 0, t))^2. \tag{74}$$

Here u is the computational solution, u_{ex} is the 'exact' solution, $N_{\mathscr{B}}$ is the number of nodes on $\mathscr{B}$, and y_m is the y-location of node m on $\mathscr{B}$. $\bar{E}(t)$ is the Eulerian norm of the error over the boundary $\mathscr{B}$. Now, for a given simulation time T, we define the global error-measure in space and time,

$$E(T) = \left(\int_0^T \bar{E}^2(t) \mathrm{d}t \right)^{\frac{1}{2}}. \tag{75}$$

This is the accumulated error on $\mathscr{B}$ during the entire simulation. Fig. 5 shows this error as a function of the simulation time T for three numerical schemes: $(N = 2, J = 2)$, $(N = 8, J = 4)$ and $(N = 17, J = 18)$. It is

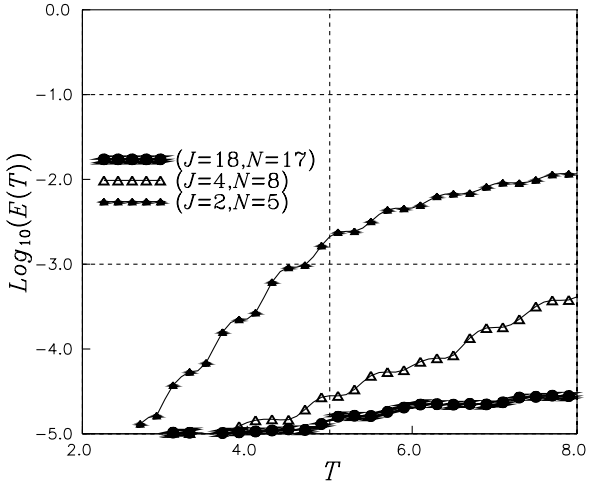

Fig. 5. The 2D wave guide problem: the global error E as a function of the simulation time T for three numerical schemes.

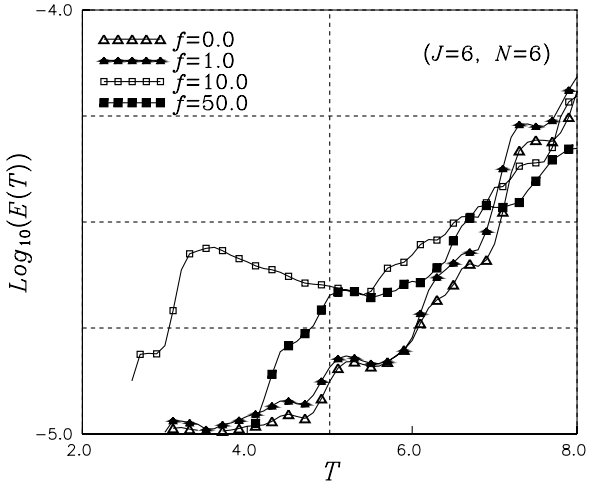

Fig. 6. The 2D wave guide problem: the global error E as a function of the simulation time T for various values of the dispersion parameter f, as obtained by the $J = N = 6$ NRBC.

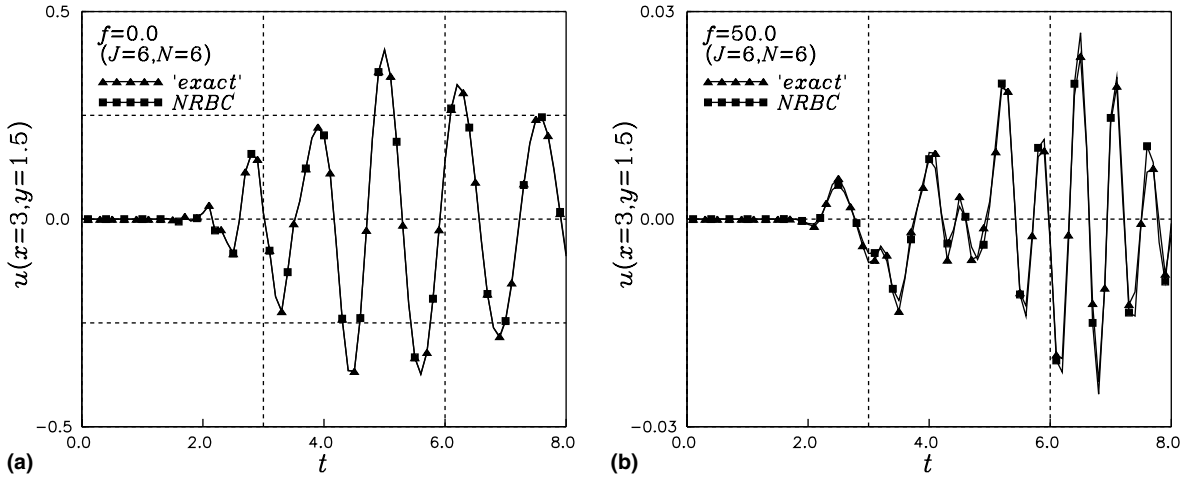

Fig. 7. The 2D wave guide problem: the solution at the center of $\mathscr{B}$ as a function of time t, for (a) $f = 0$ and (b) $f = 50$. The 'exact' solution is compared with the NRBC solution.

clear that the error reduces drastically (note the logarithmic scale) when N and J are increased. Moreover, the accumulated simulation-error increases much less rapidly with T for the higher-order schemes.

All the experiments above have been done with no medium dispersion, namely with $f = 0$. Now we fix the scheme parameters $J = N = 6$, and we look at the error for different values of the dispersion parameter f. Fig. 6 compares the $E(T)$ obtained for $f = 0$, $f = 1$, $f = 10$ and $f = 50$. For small simulation times T the error is affected significantly by the amount of dispersion, although not in a monotonic way (the $f = 10$ error is larger than the $f = 50$ error). For long simulation times all the errors are roughly on the same level. In Fig. 7 we show the solution at the point $(y = 1.5, z = 3)$, i.e., at the center of $\mathscr{B}$, as a function of time t, for $f = 0$ (Fig. 7(a)) and for $f = 50$ (Fig. 7(b)). The 'exact' solution is compared to the NRBC solution. The agreement is excellent in both cases.

7. Concluding remarks

In this paper we have derived exact DtN boundary conditions on cross-sections of 3D semi-infinite wave guides, used for truncating the guides in computations. The exact boundary condition is nonlocal in space but local in time. We showed how to incorporate it in a finite element scheme in the computational domain. Practical implementation required the truncation of the exact boundary condition by approximating an infinite sum with a finite sum, and by terminating an infinite recursion relation. The possible *dispersiveness* of the medium was treated with ease within this methodology. To the best of our knowledge, this is the first time that an exact boundary condition is derived in the dispersive time-dependent case, in any dimension.

We note, however, that the method presented here is inherently limited to *wave guides* (albeit in any dimension and with an arbitrary cross-section), since we relied on separation of variables to obtain an eigenvalue problem in the finite cross-section of a cylinder. For more general wave problems in unbounded domains one needs to resort to other methods, such as those proposed in [15,16].

We also remark that the convergence of the scheme as J (the parameter used for the termination of the recursive relation governing the auxiliary functions ϕ_j) approaches infinity has not been proved here, although numerical experiments support it. The theoretical convergence analysis is left for investigation in future studies.

Acknowledgements

This work was supported in part by the Technion's R.&M. Rosenthal Aerospace Engineering Research Fund and by the Technion's Fund for the Promotion of Research.

References

[1] D. Givoli, Exact representations on artificial interfaces and applications in mechanics, Appl. Mech. Rev. 52 (1999) 333–349.
[2] D. Givoli, Non-reflecting boundary conditions: a review, J. Comput. Phys. 94 (1991) 1–29.
[3] S.V. Tsynkov, Numerical solution of problems on unbounded domains, a review, Appl. Numer. Math. 27 (1998) 465–532.
[4] T. Hagstrom, Radiation boundary conditions for the numerical simulation of waves, Acta Numerica 8 (1999) 47–106.
[5] D. Givoli, Numerical Methods for Problems in Infinite Domains, Elsevier, Amsterdam, 1992.
[6] D. Givoli, Recent advances in the DtN finite element method for unbounded domains, Arch. Comput. Meth. Eng. 6 (1999) 71–116.
[7] L. Ting, M.J. Miksis, Exact boundary conditions for scattering problems, J. Acoust. Soc. Am. 80 (1986) 1825–1827.
[8] D. Givoli, D. Cohen, Non-reflecting boundary conditions based on Kirchhoff-type formulae, J. Comput. Phys. 117 (1995) 102–113.
[9] F. Collino, High order absorbing boundary conditions for wave propagation models. Straight line boundary and corner cases, in: R. Kleinman et al. (Eds.), Proceedings of the Second International Conference on Mathematical and Numerical Aspects of Wave Propagation, SIAM, Delaware, 1993, pp. 161–171.
[10] M.N. Guddati, J.L. Tassoulas, Continued-fraction absorbing boundary conditions for the wave equation, J. Comput. Acoust. 8 (2000) 139–156.
[11] M.J. Grote, J.B. Keller, Nonreflecting boundary conditions for time dependent scattering, J. Comput. Phys. 127 (1996) 52–65.
[12] T. Hagstrom, S.I. Hariharan, A formulation of asymptotic and exact boundary conditions using local operators, Appl. Numer. Math. 27 (1998) 403–416.
[13] I. Harari, I. Patlashenko, D. Givoli, DtN Maps for unbounded wave guides, J. Comput. Phys. 143 (1998) 200–223.
[14] D. Givoli, B. Neta, High-order non-reflecting boundary conditions for dispersive waves, Wave Motion 37 (2003) 257–271.
[15] D. Givoli, B. Neta, High-order non-reflecting boundary scheme for time-dependent waves, J. Comput. Phys. 186 (2003) 24–46.
[16] D. Givoli, B. Neta, I. Patlashenko, Finite element solution of exterior time-dependent wave problems with high-order boundary treatment, Int. J. Numer. Meth. Eng. 58 (2003) 1955–1983.
[17] R.L. Higdon, Radiation boundary conditions for dispersive waves, SIAM J. Numer. Anal. 31 (1994) 64–100.
[18] T.J.R. Hughes, The Finite Element Method, Prentice Hall, Englewood Cliffs, NJ, 1987.
[19] D. Givoli, I. Patlashenko, An optimal high-order non-reflecting finite element scheme for wave scattering problems, Int. J. Numer. Meth. Eng. 53 (2002) 2389–2411.